Supporting Information

Staykova et al. 10.1073/pnas.1102358108

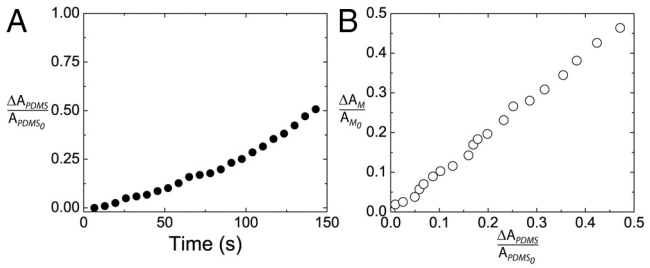

Fig. S1. Relative expansion of the polydimethylsiloxane (PDMS) and the supported bilayer. (*A*) Rate of surface area expansion of the PDMS substrate, $\Delta A_{PDMS}/A_{PDMS0}$. To estimate the area expansion of the PDMS sheet we define an initial area by some visible defects on the sheet and follow their displacement throughout the inflation. (*B*) The expansion of the PDMS sheet, $\Delta A_{PDMS}/A_{PDMS0}$ causes an equal in magnitude area expansion of the supported bilayer, $\Delta A_m/A_{m0}$. The consecutive points on the line correspond to equivolume inflation steps. The increasing distance between the points for larger area variation corresponds to an increased rate of area expansion.

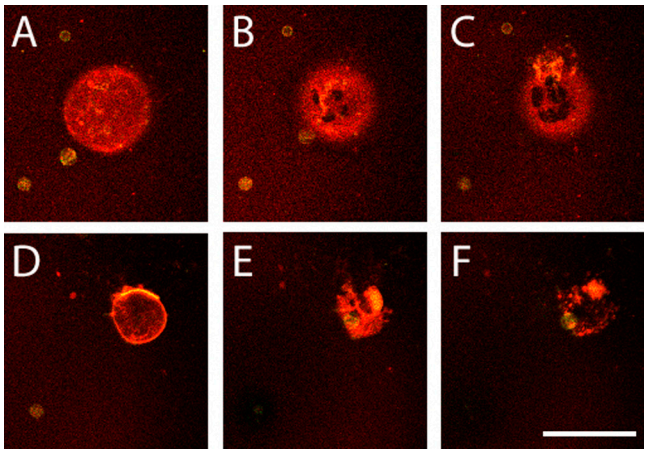

Fig. S2. Absorption of giant unilamellar vesicle (GUV) by an expanding lipid bilayer. A selection of images from the time sequence following the absorption of GUV (green) onto a supported lipid bilayer (red). Because of an exchange of lipids between GUV and the supported bilayer, GUV fluoresces also in red. (*A*) Adhesion zone between the GUV and the supported bilayer at the start of the expansion. There is a lipid flow from the vesicle to the stretched bilayer through this zone, which results in a decreasing GUV size parallel to the bilayer expansion. (*B*) Formation of several hemifusion sites in the adhesion zone between the two lipid membranes, which appear with lower fluorescent intensity. (*C*) The area of the hemifusion sites increases and the diameter of the GUV decreases with further expansion of the bilayer. The expulsion of the vesicle content in the surrounding medium is also captured. (*D*) The upper unadhered membrane of the emptied vesicle lays flat on the lower bilayer, forming a double membrane patch. The brighter fluorescence on one side of the contact rim, presumably indicates local destabilization of the membrane. (*E*) The double membrane patch disintegrates into smaller vesicles, starting from the destabilized zone. (*F*) Smaller vesicles absorb further into the expanding bilayer. Scale bar: 50 μm.

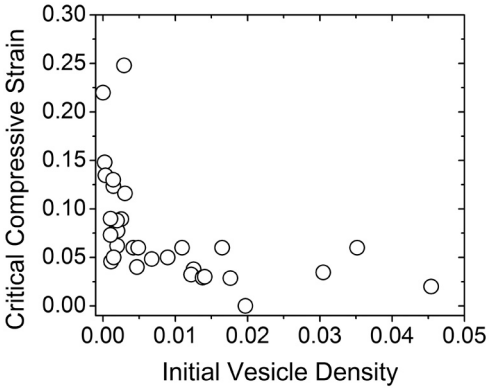

Fig. S3. Critical compressive strain for tube nucleation, as a function of the vesicle density adhered to the bilayer, at the onset of the compression. A trend is observed that supported bilayers with imperfections, i.e., many attached vesicles or lipid aggregates at sites of visual PDMS defects, tend to expel tubes at lower compressive strains.

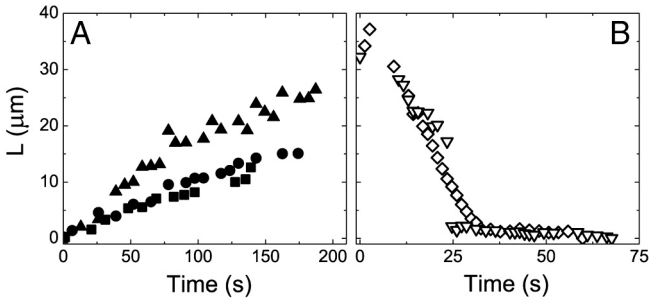

Fig. S4. Velocities of tube extraction and retraction. (*A*) Tube elongation, L (micrometers) during bilayer compression as a function of time. The average elongation velocity is about 0.4 μm/s. The decrease in the rate of tube elongation with time coincides with the decrease in the area compression rate of the bilayer (see Fig. S1*A*). (*B*) Fast retraction of tubes versus time upon the expansion of the bilayer, showing two dynamics: a gradual (diamond) and a snap-like (inverted triangle) retraction of tubes to vesicles.

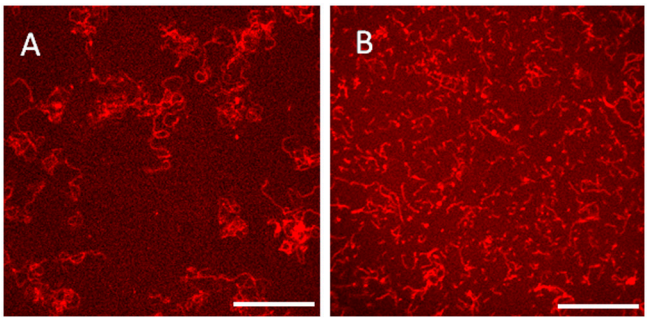

Fig. S5. Tether morphology. Two bilayers, whose surface areas have been equally compressed by 25% exhibit different tube morphologies: fewer and very long lipid tubes (*A*), or many but short tubes (*B*). Note that not all vesicles are nucleation sites for tube. Scale bar: 50 μm.